



Zhao, B., Dai, Q., Han, D., Dai, H., Mao, J., Zhuo, L., & Rong, G. (2019). Estimation of soil moisture using modified antecedent precipitation index with application in landslide predictions. *Landslides*, 16(12), 2381-2393. <https://doi.org/10.1007/s10346-019-01255-y>

Peer reviewed version

Link to published version (if available):  
[10.1007/s10346-019-01255-y](https://doi.org/10.1007/s10346-019-01255-y)

[Link to publication record in Explore Bristol Research](#)  
PDF-document

This is the author accepted manuscript (AAM). The final published version (version of record) is available online via Springer at <https://link.springer.com/article/10.1007%2Fs10346-019-01255-y#enumeration>. Please refer to any applicable terms of use of the publisher.

## University of Bristol - Explore Bristol Research

### General rights

This document is made available in accordance with publisher policies. Please cite only the published version using the reference above. Full terms of use are available: <http://www.bristol.ac.uk/red/research-policy/pure/user-guides/ebr-terms/>

1 **Estimation of soil moisture using modified Antecedent Precipitation Index**  
2 **with application in landslide predictions**

3 **Binru Zhao<sup>1,2</sup>, Qiang Dai<sup>3</sup>, Dawei Han<sup>2</sup>, Huichao Dai<sup>1</sup>, Jingqiao Mao<sup>1</sup>, Lu Zhuo<sup>2</sup>, Guiwen Rong<sup>4</sup>**

4 <sup>1</sup>College of Water Conservancy and Hydropower Engineering, Hohai University, Nanjing, China.

5 <sup>2</sup>Department of Civil Engineering, University of Bristol, Bristol, UK.

6 <sup>3</sup>Key Laboratory of VGE of Ministry of Education, Nanjing Normal University, Nanjing, China.

7 <sup>4</sup>College of Earth and Environment, Anhui University of Science and Technology, Huainan, China

8 Corresponding author: Qiang Dai ([bz17336@bristol.ac.uk](mailto:bz17336@bristol.ac.uk))

## 9 **Abstract**

10 Soil moisture plays a key role in land-atmosphere interaction systems. Although it can be estimated  
11 through in-situ measurements, satellite remote sensing and hydrological modelling, using indicators to  
12 index soil moisture conditions is another useful way. In this study, one of these indicators, The  
13 Antecedent Precipitation Index (API) is explored. Modifications were proposed to the conventional  
14 version of API by introducing two parameters to make it more in line with the physical process. First,  
15 the recession coefficient is allowed to vary with the change of air temperature, which could take into  
16 account the variation of the evapotranspiration process. Second, the API value is restricted by the  
17 maximum value of API, accounting for the maximum water holding capacity of the soil. The modified  
18 API was then calibrated and validated by comparing with the in-situ measured soil moisture. The better  
19 correlation between these two datasets demonstrates that the modified API could better indicate soil  
20 moisture conditions, compared with the conventional API. The capability of the modified API to index  
21 soil moisture conditions was further explored by applying it to landslide predictions in the Emilia-  
22 Romagna region, northern Italy. Here the recent 3-day rainfall vs the antecedent soil wetness thresholds  
23 (RS thresholds) were constructed, in which the soil wetness is indexed by the modified API. The  
24 validation of RS thresholds was carried out with the use of the contingency matrix and Receiver  
25 Operating Characteristic (ROC) curves. By comparing the prediction performance between RS  
26 thresholds and rainfall thresholds, it is found that RS threshold could provide better prediction  
27 capabilities in terms of higher hit rate and lower false alarm rate. The positive results indicate that the  
28 modified API could provide superior performance of indexing soil moisture conditions, demonstrating  
29 the effectiveness of the proposed modifications.

## 30 **1 Introduction**

31 Soil moisture in this study refers to the water content in the unsaturated zone. It plays a crucial role in  
32 the land-atmosphere interaction, through governing the water and energy balance between the land  
33 surface and the first layer of the atmosphere. As a result, the estimation of soil moisture is important in  
34 many scientific and practical issues. For rainfall-runoff modeling, the soil moisture condition prior to  
35 rainfall storms has been recognized as a key factor in determining the catchment runoff response  
36 (Brocca et al. 2010, Castillo et al. 2003, Koster et al. 2010). For numerical weather prediction and  
37 climate modelling, soil moisture is a major consideration due to its role in governing the partitioning of  
38 the mass and energy fluxes between the land and atmosphere (Bolten et al. 2010, Koster et al. 2004,  
39 Koster et al. 2009). The antecedent soil moisture is also known as an important factor in the initiation  
40 of rainfall-triggered landslides (Glade et al. 2000, Zêzere et al. 2015).

41 Soil moisture estimates can be obtained in different ways, such as in-situ measurements, remote sensing  
42 and hydrological modelling. In-situ measurements are arguably the most accurate estimation of soil  
43 moisture; however, point-based measurements make it limited in terms of spatial extent (Brocca et al.

44 2007). Due to the high cost of installation and maintenance, the in-situ measurements are not always  
45 available in the interested areas. In previous studies, the most common use of the in-situ measured soil  
46 moisture is to calibrate and test other estimates of soil moisture. Remote sensing technology has been  
47 widely used to estimate surface soil moisture in recent years (Entekhabi et al. 2010, Kerr et al. 2010),  
48 including the Soil Moisture and Ocean Salinity (SMOS) satellite launched by European Space Agency  
49 (ESA) and the Soil Moisture Active and Passive (SMAP) program scheduled by National Aeronautics  
50 and Space Administration (NASA). Many studies have evaluated and validated the remote sensed soil  
51 moisture products by comparing them with in-situ measurements (Draper et al. 2009, Gruhier et al.  
52 2009, Jackson et al. 2010, Wagner et al. 2006). They found the remote sensed soil moisture could  
53 capture soil moisture temporal variations in good agreement with in-situ measurements. The remote  
54 sensing products can provide quantitative soil moisture information at a global scale with free  
55 availabilities, and have been applied to many hydrological, meteorological and agriculture applications,  
56 despite the coarse resolution. Some attempts have also been made to estimate soil moisture with the use  
57 of hydrological modelling. Posner and Georgakakos (2015) utilized spatially distributed operational  
58 hydrological models to estimate depth-integrated soil moisture, and then applied it to a regional  
59 forecasting system for landslide hazard threat level in EI Salvador. Valenzuela et al. (2017) analyzed  
60 soil moisture conditions of 84 landslides in Asturias, NW Spain. The soil moisture was represented with  
61 the index Available Water Capacity (AWC), which is extracted from daily water balance models.  
62 Although the model-based method is a useful way to estimate soil moisture conditions, it has a high  
63 demand for data inputs and normally computationally intensive especially for larger study areas.

64 In addition to the aforementioned conventional methods, some indicators are also used as a means of  
65 estimating soil moisture. Antecedent Precipitation Index (API) is one of these indicators, proposed by  
66 Linsley et al. (1949). API is based on precipitation that has occurred over the preceding days, and due  
67 to the easier availability of the precipitation observations, the use of API is more practical for some  
68 applications where general indications of soil moisture conditions can meet demand. Crozier and Eyles  
69 (1980) employed this index to characterize the effect of antecedent soil moisture conditions on the  
70 occurrence of rainfall-triggered landslides. Crow et al. (2005) explored the effect of antecedent soil  
71 wetness on runoff forecasting with the use of API. Although API is considered as a useful indicator of  
72 soil moisture and easier to use in practical applications, deep investigations on its usage are still absent,  
73 and there are some questions remaining unexplored. For example, API is derived from the antecedent  
74 precipitation with a recession coefficient representing the rates of drainage and evapotranspiration  
75 processes. The choice of the length of the preceding period and the recession coefficient is unclear. The  
76 preceding period chosen as significant differs considerably in the previous studies (Crozier and Eyles  
77 1980, Zêzere et al. 2005), varying from 10 days to 60 days. As for the determination of the recession  
78 coefficient, most studies used the value of 0.84, which comes from Ottawa (United States) streamflow  
79 data in the work of Crozier and Eyles (1980). When defining the landslide-triggering rainfall thresholds

80 using the index for antecedent rainfall, Glade, et al. (2000) derived the recession coefficient from the  
81 recession curves of storm hydrographs for each region. The calculated thresholds show regional  
82 differences in susceptibility of a given landscape to landslide-triggering rainfall. Furthermore, there are  
83 limited investigations directly exploring the performance of API in indicating soil moisture conditions,  
84 due to the lack of in-situ measurements as the benchmark. Filling these knowledge gaps will benefit the  
85 applications of API to a wider range of practical problems.

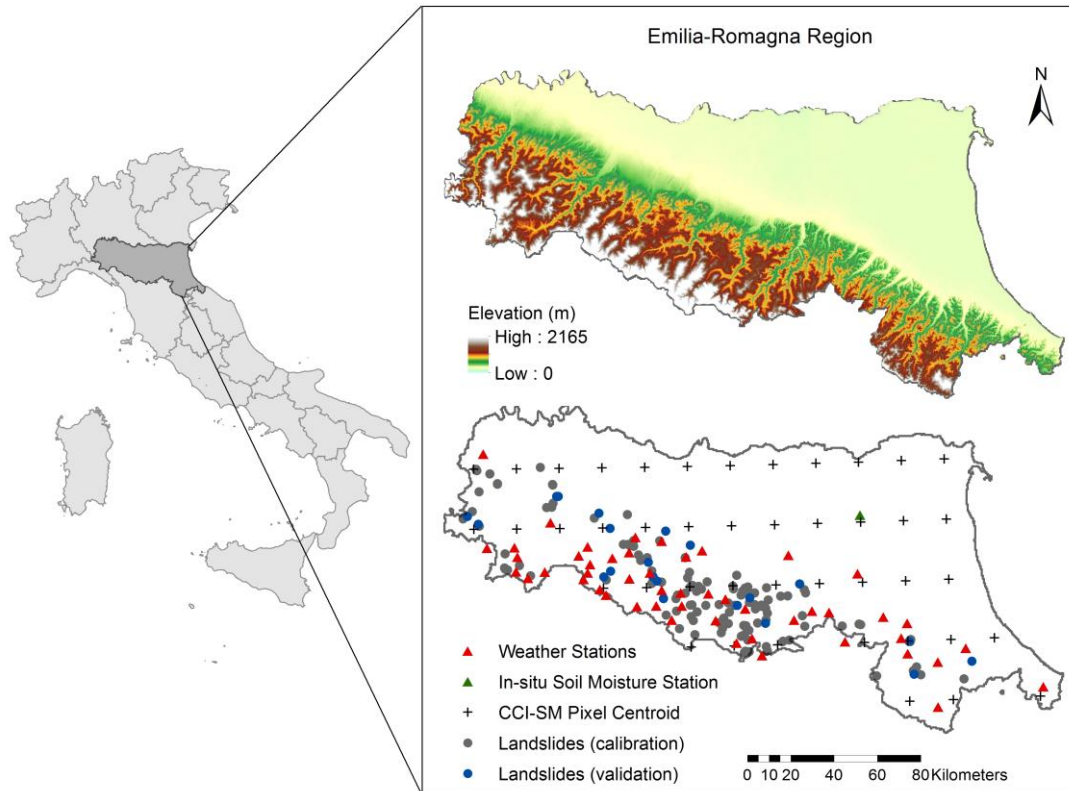
86 Based on the above, the aim of this study is to explore the improved usage of API to index soil moisture  
87 conditions. It is also attempted to modify API to make it more in line with the physical process. From  
88 a hydrological point of view, there are two aspects worth improving for API. First, in the definition of  
89 API, the recession coefficient is assumed to be constant throughout the year, ignoring the variation of  
90 the evapotranspiration process, which may be related to some factors such as temperature, wind speed,  
91 relative humidity, etc. Second, the API expression lacks the consideration of the maximum water  
92 capacity of the soil layer, which may cause an overestimation of the soil moisture. Therefore, this study  
93 intends to improve the formulation of API by incorporating more considerations of the hydrological  
94 process. The performance of API in indicating soil moisture conditions is evaluated by comparing with  
95 the in-situ measurements of volumetric water content. The application of the modified API in landslide  
96 predictions is also investigated, where the antecedent soil moisture conditions before the landslide  
97 occurrences are indexed by the modified API. This study was carried out in a northern Italian region  
98 called Emilia Romagna, owing to the availability of ample landslide records and the  
99 hydrometeorological data.

## 100 **2 Study Area and Data Sources**

### 101 **2.1 Study area**

102 The Emilia-Romagna region is located in the north of Italy, bordered by Apennines mountains (on the  
103 south and the west), Adriatic Sea (on the east) and Po River (on the north). There is a wide flat area in  
104 the northern and eastern portions of the region, while its southern and western areas are characterized  
105 by hills and mountains, whose maximum altitude is 2165m (Figure 1). This region has a typical  
106 Mediterranean climate: summer, from approximately May to October, is warm and dry, while winter  
107 from November to April is mild/cold and wet.

108 The mountainous part of the Emilia-Romagna region is extremely prone to landslides. There are a  
109 variety of landslide topologies (Martelloni et al. 2011), like the rotational-translational slides, slow earth  
110 flows, complex movements, rapid shallow landslides, etc. Although the occurrence of landslides is a  
111 result of multiple factors, in the Emilia-Romagna region, the main triggering factor of landslides is  
112 rainfall. Short but intense rainfalls are more likely to trigger debris flows and shallow landslides, while  
113 deep-seated landslides and earthflows are mainly caused by moderate but prolonged periods of rainfalls  
114 (Ibsen and Casagli 2004).



115

116 Figure 1. Location of the Emilia-Romagna region as well as the location of landslides, in-situ  
 117 measurement stations and the CCI-SM centroid pixels.

118 **2.2 Data sources**

119 In the study area there is a hydro-meteorological network maintained by Regional Agency for the  
 120 Prevention, Environment and Energy of Emilia-Romagna (Arpae), which is able to provide a variety of  
 121 observations at different temporal scales, such as rainfall, pressure, air temperature, relative humidity,  
 122 wind speed, soil moisture, etc. All these data can be obtained online  
 123 (<http://www.smr.arpa.emr.it/dext3r/>). The data used in this study was extracted the here, including the  
 124 in-situ measured soil moisture, rainfall, and temperature data.

125 There are 19 in-situ soil moisture measurement sites within the study area, where Time Domain  
 126 Reflectometry (TDR) equipped with dataloggers is used to measure soil water content at different soil  
 127 depths. Among these sites, only the San Pietro Capofiume site (marked with the green triangle in Figure  
 128 1) could provide long-term surface soil moisture observations (at 10 cm soil depth). Therefore, this site  
 129 was selected to explore the performance of API, where data of the daily average temperature, daily  
 130 cumulative rainfall and soil water content are needed. Considering the completeness of the required  
 131 data, data of the period from 2006 to 2016 were extracted and used for the analysis.

132 For the purpose of applying the modified API to landslide predictions, the modified API was calculated  
 133 for the landslide-prone area of the Emilia-Romagna region, and its validation needs to be evaluated

134 using the in-situ soil moisture measurements. However, due to the lack of long-term in-situ measured  
135 soil moisture in this area, remote sensed soil moisture was utilized as a proxy. The modified API was  
136 calculated based on the data from 50 weather stations (marked with red triangles in Figure 1) for the  
137 period from 2006 to 2016. The remoted sensed soil moisture adopted in this study is the state-of-the-art  
138 ESA Climate Change Initiative (CCI) soil moisture product (CCI-SM hereafter). This product is  
139 produced by merging information from multiple active and passive microwave sensors, including three  
140 harmonized satellite soil moisture datasets: a merged ACTIVE (1991-2016), a merged PASSIVE (1978-  
141 2016) and a COMBINED (1978-2016). The soil moisture information provided by the CCI-SM product  
142 is the volumetric water content ( $m^3/m^3$ ), with a daily temporal resolution, and 0.25-degree spatial  
143 resolution. In this study, the latest version (v04.2, released in early 2018) of CCI-SM COMBINED  
144 product was employed, whose pixel centroids are shown in Figure 1.

145 The landslide data was collected from Emilia-Romagna Geological Survey, an agency maintaining a  
146 catalogue of historical landslides in the Emilia-Romagna region. The landslides recorded in this  
147 catalogue were from various sources, such as reports to local authorities, national and local press,  
148 technical documents. Most landslides that led to casualties and damage were recorded, while those with  
149 little influence or damage were more likely to be undetected. In general, a range of landslide occurrence  
150 information should be gathered, such as location, date, accuracy level of the record, characteristics  
151 (length, width, type and material), triggering factors, damage and references. However, in practice, it is  
152 difficult to collect and record all the above information. For most landslides, only the occurrence  
153 location and date were recorded. Despite such a fact, this catalogue is the most complete and detailed  
154 records of landslides in the Emilia-Romagna region, and regarded as a proxy of actual landslides (Rossi  
155 et al. 2010). In this study, only the landslides with daily accuracy in terms of the occurrence date were  
156 selected for the landslide prediction analysis, with a total of 140 (Figure 1). The landslides occurred  
157 during the period from 2006 to 2014 were used to establish the thresholds for landslide occurrence, and  
158 the landslides in the period from 2015 to 2016 were for the validation of the thresholds.

### 159 **3 Methods**

#### 160 **3.1 Antecedent Precipitation Index**

161 Antecedent Precipitation Index (API) is an index derived from the preceding daily rainfall, regarded as  
162 a simple surrogate measure of soil moisture. One common definition of API was proposed by Fedora  
163 (1987) to simulate storm hydrographs in the Oregon Coast Range, written as:

$$API_t = k API_{t-\Delta t} + P_{\Delta t} \quad (1)$$

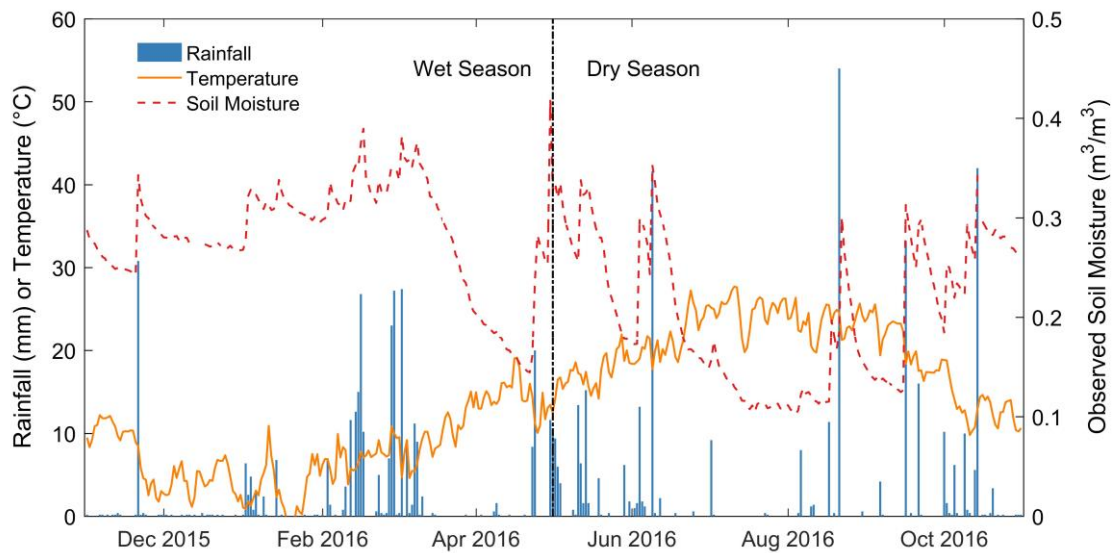
164 where  $API_t$  is the API at time  $t$ ,  $P_{\Delta t}$  is the cumulative precipitation during the period from  $t - \Delta t$  to  $t$  (in  
165 this study  $\Delta t = 1$  day), and  $k$  is the recession coefficient, which is assumed constant throughout the  
166 year.

167 From a hydrological point of view, there are two aspects worth improving for the above formulation of  
168 API. First, assuming the recession coefficient is a constant is not in agreement with the physical process.  
169 The recession coefficient is adopted to characterize the rate of water loss, which is a result of the  
170 drainage and evapotranspiration processes. Considering that the evapotranspiration process is  
171 dependent on multiple factors (e.g. air temperature, wind speed, relative humidity) and these factors  
172 vary through the year, assuming the recession coefficient is a constant ignores the variation of these  
173 factors and their effects on soil moisture conditions. The effect of temperature on the soil moisture  
174 evolution can be found in Figure 2, which illustrates the temporal evolution of in-situ soil moisture  
175 measurements in the San Pietro Capofiume site as well as the corresponding rainfall and temperature  
176 series. As can be seen, for three dry periods (December of 2015, March and April of 2016 and July of  
177 2016), their rainfall conditions are similar, with little or zero amount. However, their soil moisture  
178 conditions show significant differences. For December of 2015, the soil remains in a wetter condition,  
179 while for other two dry periods, the water content is lower. This can be explained by the difference of  
180 the temperature during these periods. Higher temperature conditions benefit the evapotranspiration  
181 process and lead to a more loss of water, thus less water is attributed to the soil resulting in a lower  
182 water content. On the contrary, lower temperature conditions will result in the wetter soil conditions  
183 due to the reduced water loss. Therefore, it is necessary to take into account the variation of some factors  
184 that affect the evapotranspiration process. Due to the easier availability of temperature data, only  
185 temperature is considered in this study. For this purpose, the formulation of API expressed in Equation  
186 (1) is modified by allowing the recession coefficient to vary according to the change of temperature. As  
187 a line relationship is simpler and easy to implement, the variation of the recession coefficient is assumed  
188 as linear in this study:

$$k = 0.84 + \delta (20 - T_{ave}) \quad (2)$$

189 where  $T_{ave}$  is the daily average temperature ( $^{\circ}\text{C}$ ) and  $\delta$  is a sensitivity parameter ( $^{\circ}\text{C}^{-1}$ ). When  $\delta$  is  
190 equal to 0, the recession coefficient is constant as 0.84, which is widely used in the previous studies,  
191 recommended by Crozier and Eyles (1980). The reason for using  $20^{\circ}\text{C}$  as the basis is that it is the most  
192 common temperature when the value of 0.84 is used.





193

194 Figure 2. Time series of in-situ soil moisture measurements in the San Pietro Capofiume site as well  
 195 as the corresponding rainfall and temperature series.

196 Second, the API expression lacks the consideration of the maximum water capacity of the soil layer. In  
 197 the hydrological process, prolonged rainfall will saturate the soil allowing no additional water to be  
 198 held. As a result, any additional rainfall that falls becomes overland flow. This process is termed as  
 199 saturation excess overland flow. In this case, API calculated with Equation (1) will overestimate the  
 200 water content in the soil. Therefore, a parameter  $API_{max}$  is introduced to take into account the process  
 201 of saturation excess overland flow: when the value of API exceeds  $API_{max}$ , it is equal to  $API_{max}$ .

202 The optimization of the parameter  $\delta$  and  $API_{max}$  is carried out by comparing the modified API with the  
 203 observed soil moisture for the period from 2006 to 2013. As the modified API attempts to capture soil  
 204 moisture temporal variations in good agreement with in-situ measurements, Pearson correlation  
 205 coefficient is used as the evaluation criterion to measure the linear correlation between the modified  
 206 API and the measured soil moisture. Pearson correlation coefficient ranges from -1 to 1, where 1 is total  
 207 positive linear correlation, 0 is no linear correlation, and -1 is total negative linear correlation. The  
 208 optimized parameters are then validated for the period from 2014 to 2016. Due to the lack of in-situ  
 209 measured soil moisture, it is difficult to determine the optimal parameters for other locations. It is  
 210 assumed that it is feasible to extrapolate the parameters at the San Pietro Capofiume site to the whole  
 211 study area. In order to assess the reliability of this assumption, the modified API series is compared  
 212 with the CCI-SM product for each weather station.

### 213 3.2 Rainfall versus soil wetness threshold

214 A recent rainfall versus antecedent soil wetness threshold (hereafter RS threshold) is employed to  
 215 explore the application of API in landslide prediction studies. The soil wetness here is the quantification  
 216 of the soil moisture condition. RS threshold consists of two components: one is the recent 3-day

217 cumulative rainfall (R) before the landslide occurrence, and the other is the antecedent soil wetness of  
218 the day preceding the recent 3-day (S), which is indexed by the modified API as proposed. The modified  
219 API here is scaled with the maximum and minimum value, thus ranging from 0 to 1 with higher values  
220 corresponding to wetter soil conditions.

221 For the purpose of constructing and testing RS threshold, all datasets are divided into two periods: 2006-  
222 2014 for the construction of RS threshold, and 2015-2016 for the evaluation of the threshold. RS  
223 threshold is determined by various combinations of the critical value of landslides' rainfall and soil  
224 wetness, which are defined with their different percentiles. Taking the rainfall's 5th percentile (P5) as  
225 an example, it means there are 5% landslides with the recent 3-day cumulative rainfall value less than  
226 P5. The two components of the RS threshold are used separately in this study: the critical value of the  
227 antecedent soil wetness is firstly used as a criterion and then the critical value of rainfall is used. The  
228 reason of not constructing the functional relation between these two components (like the power law  
229 relation between rainfall intensity and rainfall duration in the rainfall threshold) is because this  
230 relationship remains unknown, although there are some studies assuming it as the linear relation  
231 (Chleborad et al. 2008, Mirus et al. 2018, Scheevel et al. 2017). The landslide occurrence is predicted  
232 only when these two components' critical values are exceeded. The prediction performance of different  
233 thresholds is evaluated with the help of the contingency matrix and Receiver Operating Characteristic  
234 (ROC) curves. This is the most common manner used in landslide early warning studies (Gariano et al.  
235 2015, Mirus, et al. 2018, Staley et al. 2013).

236 Hit Rate (HR) is also known as the true positive rate, and used to measure the proportion of landslides  
237 that are correctly predicted:

$$HR = \frac{TP}{TP + FN} \quad (3)$$

238 False Alarm Rate (FAR) is also known as the false positive rate, and used to measure the proportion of  
239 false alarms over the events when no landslide occurs:

$$FAR = \frac{FP}{FP + TN} \quad (4)$$

240 In Equations (3) and (4), True Positive (TP), False Negative (FN), False Positive (FP) and True Negative  
241 (TN) are four possible outcomes of the thresholds' prediction results. TP means the threshold predicts  
242 landslide occurrences successfully; FN is an error where the threshold does not predict the occurrence  
243 of landslides; however, in reality landslides occur; FP is an error where the threshold predicts the occurs  
244 of landslides; however, there is no landslide occurrence in reality; TN means the threshold correctly  
245 predicts the non-occurrence of landslides.

246 The value of HR and FAR ranges between 0 and 1. When HR is equal to 1 and FAR is equal to 0, the  
247 optimal performance is achieved. This is referred to a perfect point. For the better measurement of the  
248 gap to the perfect point, the Euclidean distance (d) is also calculated for each threshold scenario. The  
249 smaller the distance, the better the prediction performance.

$$d = \sqrt{(\text{FAR})^2 + (\text{HR} - 1)^2} \quad (5)$$

### 250 **3.3 Rainfall threshold**

251 In order to directly compare the prediction performance of RS threshold with that of the rainfall  
252 threshold, the cumulative event rainfall E (mm) versus rainfall duration D (day) threshold was also  
253 constructed using the Frequentist approach proposed by Brunetti et al. (2010). They assumed the general  
254 formulation of threshold curves as a power law:

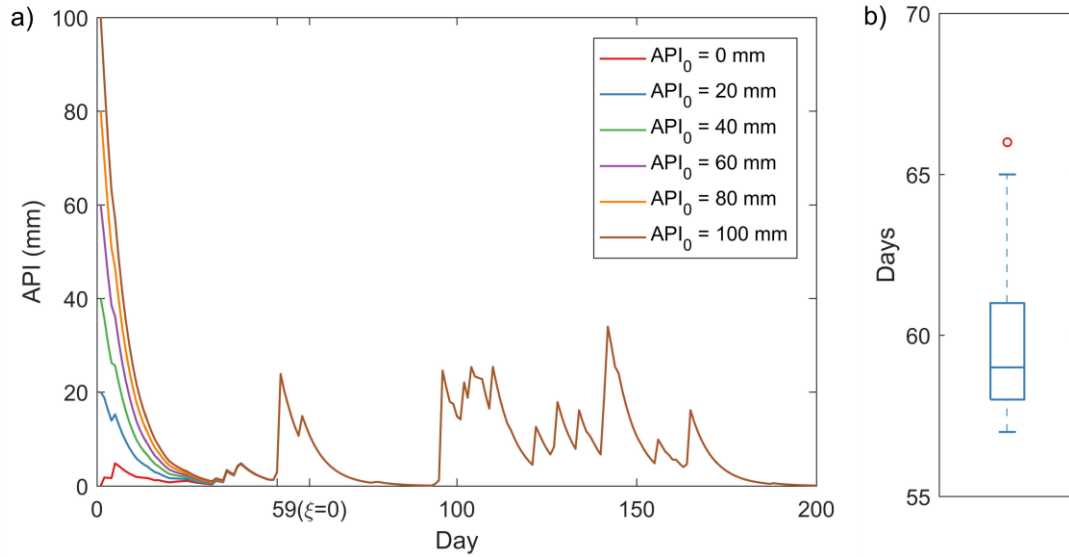
$$E = \alpha \cdot D^\gamma \quad (5)$$

255 where  $\alpha$  is a scaling constant (the intercept at the value of D equal to 1),  $\gamma$  is the shape parameter  
256 (defining the slope of the power law curve). The cumulative rainfall E (mm) and rainfall duration D  
257 (day) are calculated based on rainfall events, which are identified using the automatic procedure  
258 proposed by Melillo et al. (2014). Thresholds with different percentiles are calculated and evaluated.  
259 The data used for the construction and test of rainfall thresholds are the same as that for RS thresholds,  
260 and the evaluation method also remains the same.

## 261 **4 Results**

### 262 **4.1 The effect of the initial value**

263 Before using Equation (1) to calculate API, it was necessary to explore the effect of the initial value  
264 and the determination of the period length for recursion, as the expression of API in Equation (1) is a  
265 recursive form. For this purpose, different initial values were designed ranging from 0 to 100 mm. Once  
266 the initial value is given, the expression in Equation (1) was run for the next 200 days. The temporal  
267 evolution of API with different initial values is shown in Figure 3a. It is clear to see whatever the initial  
268 value is, the value of API after near 60 days remains the same, although there is a distinct difference in  
269 the first 20 days. In other words, the effect of initial value decreases and becomes insignificant after the  
270 60<sup>th</sup> day. In order to exclude the influence of the position of the initial day, the above procedure was  
271 repeated by choosing different dates as the initial day. Here 366 days of the year 2012 were used for  
272 analysis. It is found that the day no longer affected by the initial value distributes in the range from the  
273 57<sup>th</sup> to 65<sup>th</sup> day, with the median value as the 59<sup>th</sup> day (Figure 3b). Based on the above results, API was  
274 calculated with the initial period of 60 days, after which the initial value has no longer effect on the API  
275 value. In this study, 30 mm was used as the initial value, which is the average level of API.



276

277

278

Figure 3. The effect of the initial value, a) time series of API with different initial values, b) the distribution of the day no longer affected by the initial value.

279

#### 4.2 The modified API

280

281

282

283

284

285

286

287

288

289

290

291

292

293

294

295

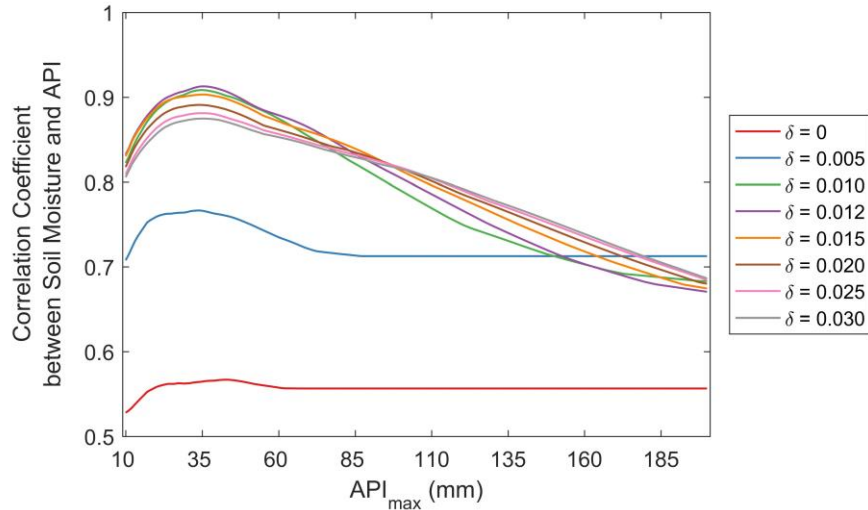
296

297

298

299

Two parameters  $\delta$  and  $API_{max}$  were introduced to modify API. To optimize these two parameters, different combinations of  $\delta$  and  $API_{max}$  were tested. Their performance was evaluated with the use of Pearson correlation coefficient ( $r$ ), which was calculated using the modified API series and the observed soil moisture series of the period from 2006 to 2013. To make the recession coefficient greater than 0.5, considering the variation range of the temperature, the sensitive parameter  $\delta$  ranging from 0 to 0.03 was explored. As for  $API_{max}$ , if a too small value is used as  $API_{max}$ , API remains the same as  $API_{max}$  for most cases, which is not consistent with the reality. Here 10 mm was considered as the lower limit of the variation range. Given the maximum value of API, the upper limit of the variation range was determined as 200 mm. Some representative results are shown in Figure 4. As  $API_{max}$  is regarded as an indirect measure of water capacity of the soil, it should remain constant for a particular type of soil. Therefore, the value of  $API_{max}$  is firstly determined for the study site. It is interesting to find that for all values of  $\delta$ , the correlation coefficient between soil moisture and API has the best value when  $API_{max}$  is around 35 mm. Therefore, 35 mm is selected as the optimal value of  $API_{max}$ . In the case of  $API_{max}$  as 35 mm, it is clear that the correlation coefficient increases greatly when  $\delta$  changes from 0 to greater than 0, indicating that the performance of API could be improved by allowing the recession coefficient to vary with the temperature. The improvement is obvious when  $\delta$  changes from 0 to 0.01, with the correlation coefficient increasing from around 0.55 to near 0.9. However, after  $\delta$  larger than 0.01, increasing the value of  $\delta$  no longer results in the significant improvements and even worsens of the correlation coefficient, and the optimal result is reached at  $\delta$  as 0.012. As a result, the optimal value of  $\delta$  is selected as 0.012.



300

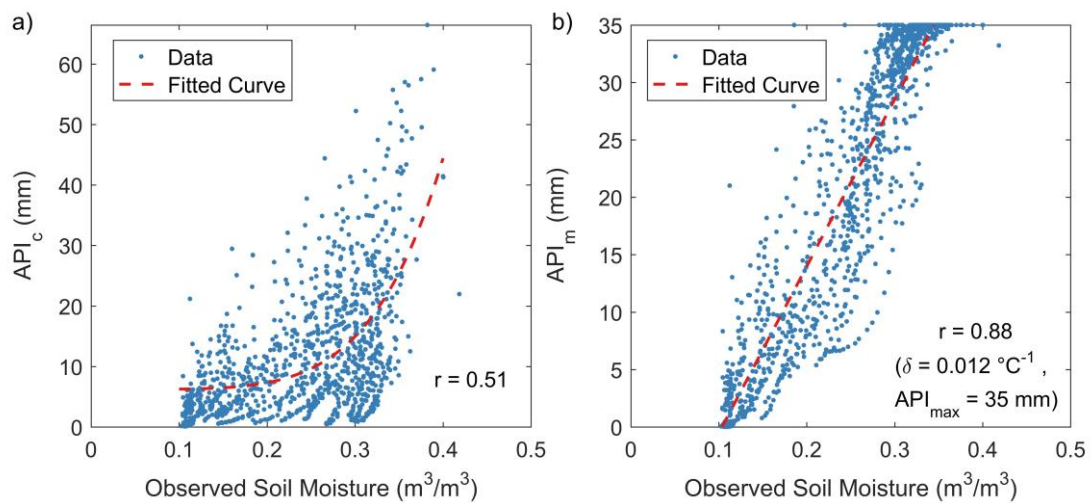
301

Figure 4. The optimization of parameters  $\delta$  and  $API_{max}$ .

302

To validate the optimized parameters, an evaluation of the modified API during the independent period from 2014 to 2016 was carried out. The scatter plot of API against the observed soil moisture as well as the fitted curve is shown in Figure 5 for both versions of API. Hereafter, the conventional API is represented by  $API_c$ , and the modified API is represented by  $API_m$ . From Figure 5a, the linear correlation relationship between the observed soil moisture and  $API_c$  is insignificant, and it is found that a power function has the best fit to the data points. As for Figure 5b,  $API_m$  has a significant linear positive relationship with observed soil moisture values, with Pearson correlation coefficient increasing from 0.51 to 0.88. This not only indicates that the calibrated parameters' performance is reliable for the independent period, but also demonstrates that introducing two parameters to  $API_c$  really improves the API's performance of indicating soil moisture conditions.

311



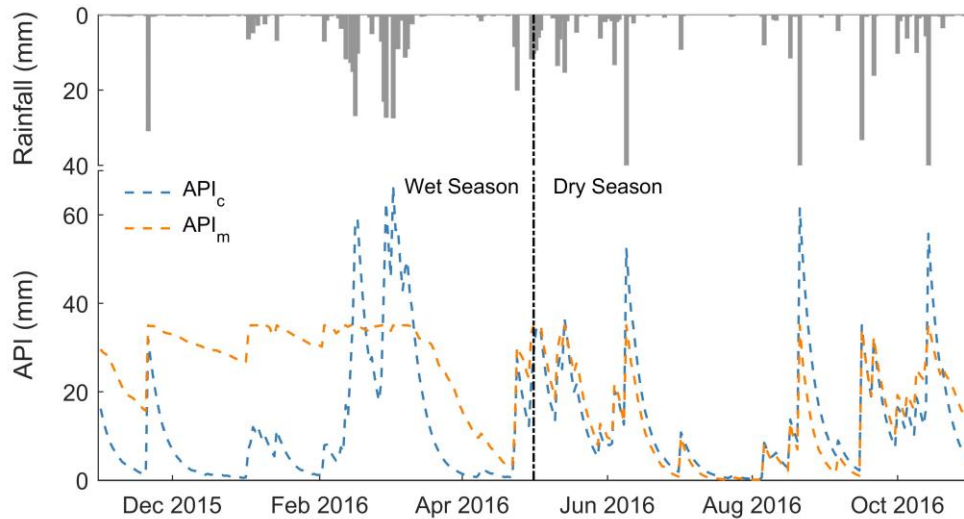
312

313

Figure 5. The scatter plot of API against the observed soil moisture as well as the fitted curve, a) for

314

$API_c$ , b) for  $API_m$ .



315

316 Figure 6. Time series of  $API_c$  and  $API_m$  as well as rainfall for the period from November 2015 to  
 317 October 2016.

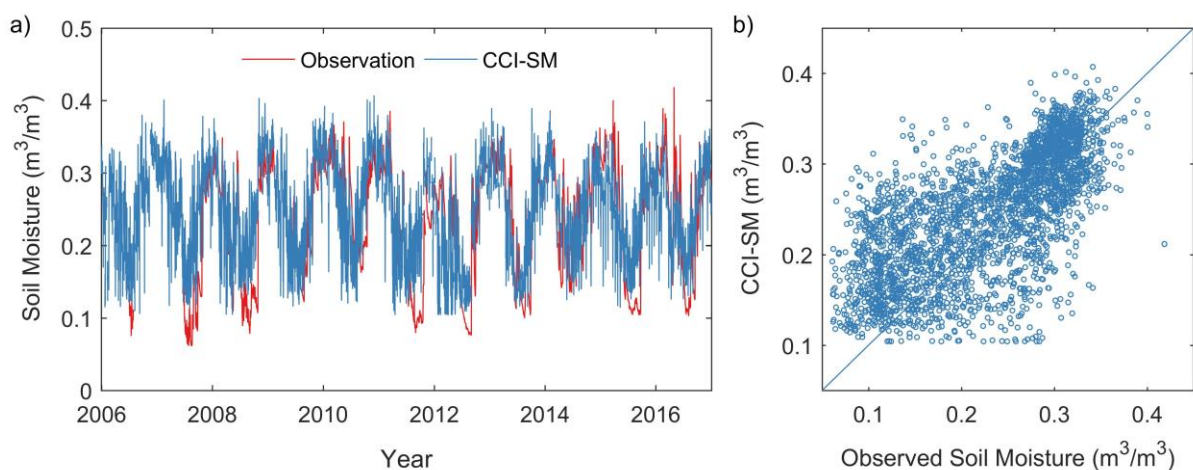
318 For better demonstrating the superior performance of  $API_m$ , the temporal evolution of  $API_c$  and  $API_m$   
 319 as well as rainfall are illustrated in Figure 6. As expected, the change pattern in terms of increase or  
 320 decrease is the same for these two variables, because the decrease or increase of API is mainly related  
 321 to the variation of rainfall. For instance, during the period with rainfall, the soil conditions become  
 322 wetter, represented by an increase in the value of API. As for the period with little or no rainfall, the  
 323 soil conditions become drier, represented by a decrease in their values. Despite the same change  
 324 direction,  $API_c$  and  $API_m$  show distinct differences in terms of change degree and change range. The  
 325 change degree is more dependent on the contribution of the antecedent rainfall, while the change range  
 326 is related to the maximum water capacity of the soil. For the wet season from November 2015 to April  
 327 2016, the difference between  $API_c$  and  $API_m$  is distinct, which could be explained by the two  
 328 parameters introduced to  $API_m$ . The parameter  $\delta$  leads to a higher  $k$  owing to the lower temperature in  
 329 the wet season, resulting in a more contribution of the antecedent rainfall. Therefore, for the period with  
 330 little or no rainfall, the value of  $API_m$  will not decrease as quickly as the  $API_c$ . As for the period with  
 331 intense rainfall, the value of  $API_m$  is restricted by  $API_{max}$ , leading to the difference in terms of change  
 332 range. For the dry season from May 2016 to October 2016, the biggest difference between  $API_c$  and  
 333  $API_m$  is the change range caused by the introduction of  $API_{max}$ . As for the change degree that is  
 334 influenced by  $\delta$ , there is no distinct difference. The reason is that during this period, the temperature is  
 335 near or a little greater than  $20^\circ\text{C}$ , therefore the  $k$  value is similar in both expressions of  $API_m$  and  $API_c$ ,  
 336 and thus they have similar change degree.

### 337 4.3 Parameter Extrapolation

338 To apply the modified version of API to landslide prediction studies, the values of  $API_m$  are required,  
 339 whose calculation requires the determination of the two added parameters. However, due to the lack of

340 in-situ measured soil moisture in the landslide-prone area, it is difficult to optimize them in the same  
341 way as that used in the San Pietro Capofiume site. Therefore, it is assumed that it is feasible to  
342 extrapolate the parameters at the San Pietro Capofiume site to the whole study area. In order to validate  
343 the parameter extrapolation, the  $API_m$  series was assessed with the CCI-SM product for each weather  
344 station. Here Pearson correlation coefficient was used as the criterion. The reason for not using CCI-  
345 SM to calibrate parameters for the study area is that there are uncertainties associated with the satellite  
346 data, which will lead to more uncertainties to the determination of parameters and the calculation of  
347  $API_m$ . Therefore, the CCI-SM product is only used for evaluating the parameter extrapolation.

348 Before using CCI-SM product, its reliability and accuracy were firstly investigated. The CCI-SM series  
349 is compared with the in-situ measured soil moisture in the San Pietro Capofiume site for the period  
350 from 2006 to 2016, which are shown in Figure 7. It can be seen from Figure 7a, CCI-SM is able to  
351 capture the overall seasonal and temporal variations of soil moisture. Despite this, it is noted that there  
352 are periods that CCI-SM product shows wetter conditions than the observed. Figure 7b presents the  
353 scatter plot of CCI-SM against the observed soil moisture. The variation range for both datasets are  
354 similar, CCI-SM ranges between 0.1 and 0.4  $m^3/m^3$ , and the observed soil moisture varies from 0.05 to  
355 0.43  $m^3/m^3$ . Moreover, although for some dry conditions (e.g., the observed soil moisture is between  
356 0.05 to 0.25), CCI-SM product overestimates the soil moisture, in general, the data are distributed  
357 mainly around the identical line. The Pearson correlation coefficient of 0.68 also indicates the CCI-SM  
358 is generally in line with the in-situ measurements. In summary, despite some drawbacks of CCI-SM, it  
359 is considered acceptable to represent the temporal evolution of soil moisture conditions and can be used  
360 for the validation of the parameter extrapolation.

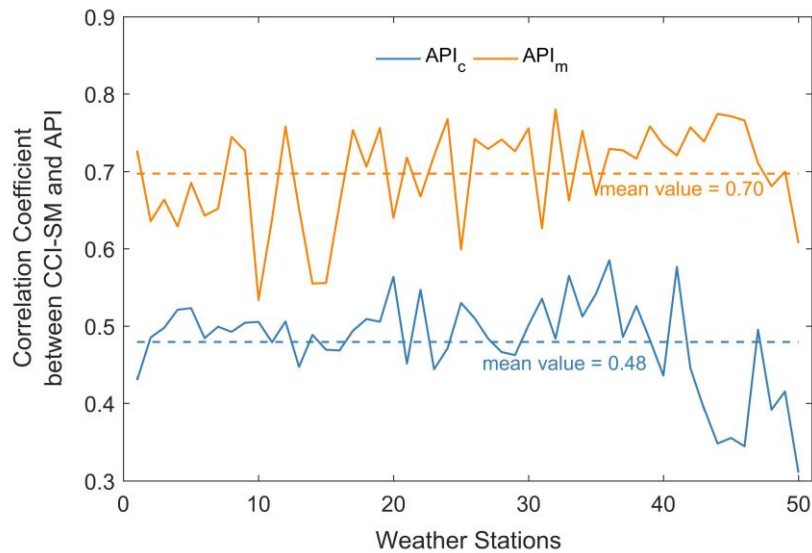


361  
362 Figure 7. Comparison between the observed soil moisture and CCI-SM product, a) the time series  
363 plot, b) the scatter plot with the identical line.

364



365 The validation of the parameter extrapolation was carried out for 50 weather stations within the study  
 366 area. For each station,  $API_m$  of the period from 2006 to 2016 was calculated based on its rainfall and  
 367 temperature datasets, with the use of those two parameters optimized in the San Pietro Capofiume site.  
 368 By matching the nearest CCI-SM pixel to the station, the CCI-SM dataset can be extracted. With the  
 369  $API_m$  and CCI-SM datasets, the Pearson correlation coefficient was calculated as the evaluation  
 370 criterion. For the purpose of comparison, the same process was also carried out for  $API_c$ . The value of  
 371 correlation coefficient is shown in Figure 8. As is seen, the performance of the parameter extrapolation  
 372 varies with stations, with the minimum as 0.53 and the maximum as 0.78. In spite of the variance of the  
 373 performance,  $API_m$  shows a great improvement over  $API_c$  by comparing the mean value of their  
 374 correlation coefficients (growing from 0.48 to 0.70). Although the value of the correlation coefficient  
 375 is not great enough, given the uncertainties associated with the CCI-SM product, the performance of  
 376 the parameter extrapolation is regarded as acceptable and  $API_m$  can be used as an indicator for soil  
 377 moisture conditions in the study area.



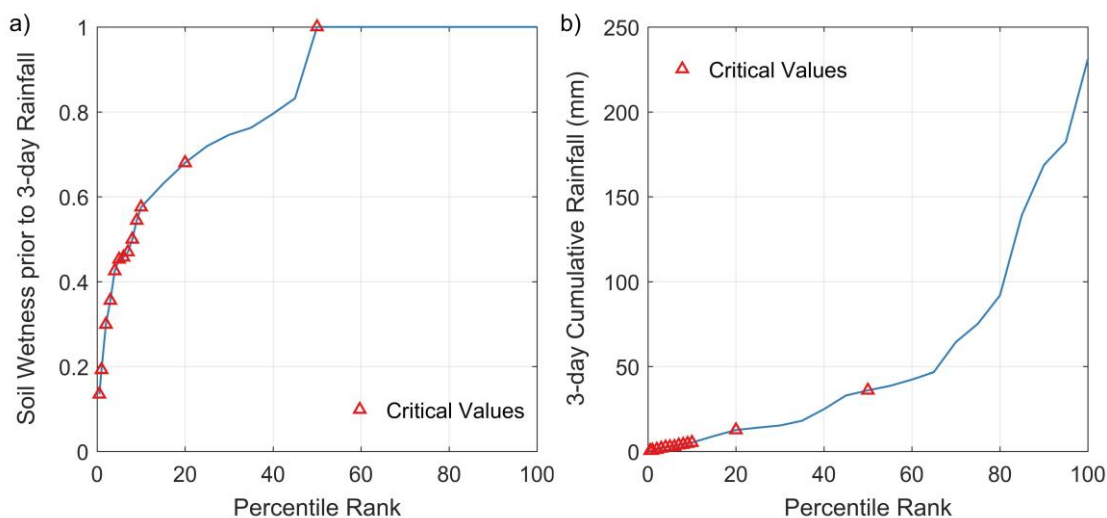
378  
 379 Figure 8. The correlation coefficient between CCI-SM and two versions of API for 50 weather  
 380 stations as well as their mean values.

381 **4.4 The application of  $API_m$**

382 To further evaluate the performance of  $API_m$  in indicating soil moisture conditions, an investigation  
 383 was carried out to apply it in landslide prediction studies. Here RS threshold was constructed using the  
 384 rainfall and soil wetness information associated with the occurrence of landslides during the period  
 385 from 2006 to 2014. For RS threshold, the rainfall indicator is the recent 3-day cumulative rainfall (R)  
 386 before the landslide occurrence, and the antecedent soil wetness (S) is indexed by the  $API_m$  of the day  
 387 before the recent 3-day. Here the value of  $API_m$  is scaled with its minimum and maximum values,  
 388 ranging from 0 to 1. With the rainfall and soil wetness information of all landslides, RS threshold is



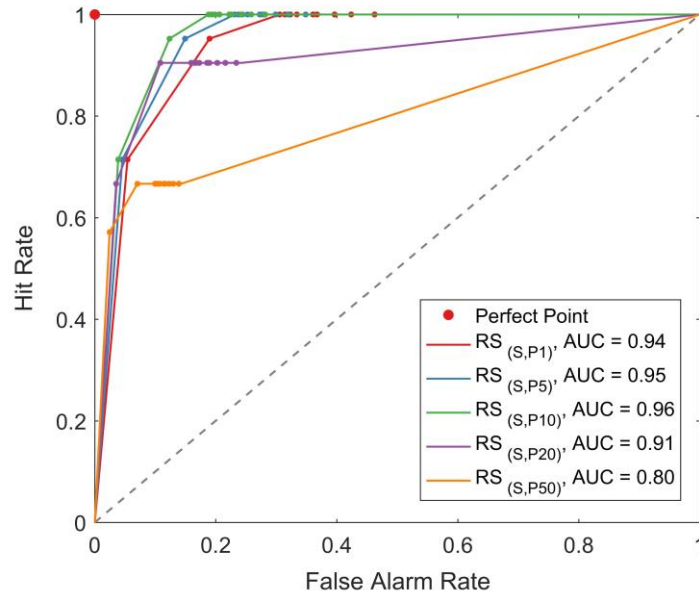
389 determined by various combinations of these two variables' critical values, which are defined at their  
 390 different percentiles (1, 2, 3, 4, 5, 6, 7, 8, 9, 10, 20 and 50). The percentile distribution of all landslides'  
 391 antecedent soil wetness and recent rainfall is shown in Figure 9, where the critical values of these two  
 392 variables are marked with red triangles. From Figure 9a, the antecedent soil condition for more than 80%  
 393 of landslides is more than 0.68, while more than 50% of landslides have antecedent soil wetness equal  
 394 to 1. As for the recent 3-day cumulative rainfall in Figure 9b, it is found there are always rainfall before  
 395 the landslide occurrence, although the rainfall amount varies a lot. More than 50% of landslides have  
 396 the recent 3-day cumulative rainfall greater than 36 mm. The big difference of the antecedent soil  
 397 wetness and 3-day cumulative rainfall of landslides is the reason why various percentiles are  
 398 investigated.



399  
 400 Figure 9. The percentile distribution of all landslides' antecedent soil wetness and recent 3-day  
 401 cumulative rainfall (soil wetness is indexed with the scaled value of  $API_m$ ).

402 The prediction performance of different RS thresholds was evaluated using the data from 2015 to 2016,  
 403 whose ROC curves are shown in Figure 10. In this figure, the point represents one scenario of RS  
 404 threshold, determined by one combination of the critical value of soil wetness and rainfall. The critical  
 405 value of soil wetness remains the same for the points on the same curve, for instance, the critical value  
 406 of soil wetness is determined with its 1st percentile (P1) for the points on the red curve. The difference  
 407 among the points on the same curve is the rainfall's critical value, from right to left, the rainfall's critical  
 408 value is determined by 12 different percentiles at the percentile rank of 1, 2, 3, 4, 5, 6, 7, 8, 9, 10, 20  
 409 and 50. It can be seen from Figure 10, when the critical value of the antecedent soil wetness remains  
 410 the same, increasing the critical value of the recent 3-day cumulative rainfall could improve the false  
 411 alarm rate sometimes at the expense of reducing the hit rate. This result also applies to the case in which  
 412 the rainfall's critical value remains the same and the soil wetness' critical value increases. In order to  
 413 determine the optimal critical value of the antecedent soil wetness, the area under the ROC curve (AUC)  
 414 is employed, the larger the area, the better the prediction performance. Based on the value of AUC, the

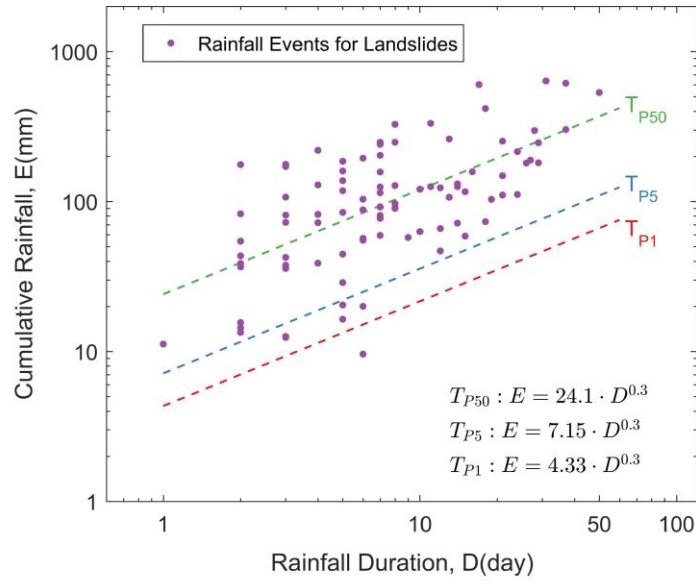
415 critical value of the soil wetness determined with the 10th percentile could provide the best predictive  
 416 capabilities (relative higher hit rates and lower false alarm rates), which is used to compare with the  
 417 rainfall threshold's performance.



418

419 Figure 10. Receiver operator characteristic (ROC) curves for various RS thresholds with the area  
 420 under the curve (AUC) listed (" S, Pi " means the critical value of the antecedent soil wetness is  
 421 determined with the ith percentile).

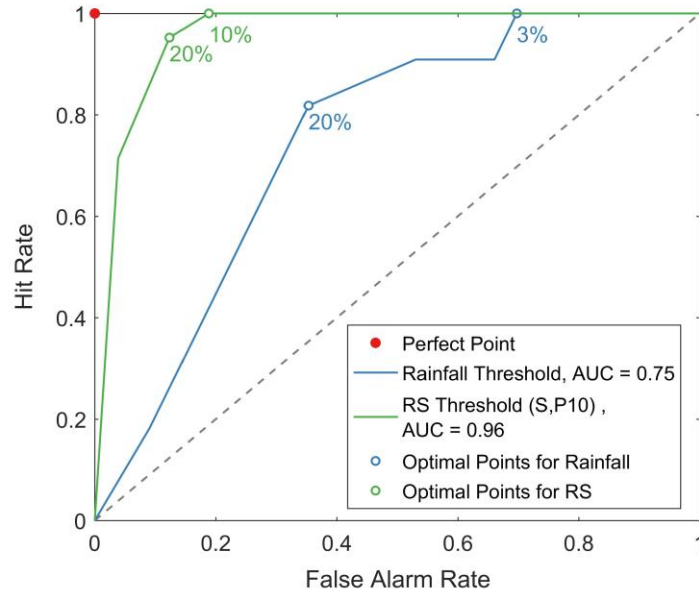
422 The rainfall thresholds with different percentile ranks were determined for comparison (Table 1a).  
 423 Three thresholds with the 1st, 5th and 50th percentiles are shown in Figure 11 as well as the rainfall  
 424 conditions (D, E) that are likely to trigger landslides. Rainfall conditions associated with landslides are  
 425 in the range of duration  $1 \text{ day} \leq D \leq 50 \text{ days}$ , and in the range of cumulative event rainfall  $9.6 \text{ mm} \leq$   
 426  $E \leq 637.2 \text{ mm}$ , which are the ranges of validity for the threshold. Taking the percentile rank of 5 as an  
 427 example, as expected, there are 5 pairs of the (D, E) data (5% of 112 rainfall conditions) below the P5  
 428 threshold. It is noted that the uncertainties of the thresholds depend on the number and distribution of  
 429 the empirical data, and increasing the sample size could reduce the uncertainties.



430

431 Figure 11. The rainfall thresholds with percentile ranks of 1, 5 and 50, as well as the rainfall  
 432 conditions (D, E) that are likely to trigger landslides.

433 The ROC curves are plotted in Figure 12 for rainfall thresholds and RS thresholds whose soil wetness's  
 434 critical value is determined with the 10th percentile. The statistical indicators of those thresholds are  
 435 summarized in Table 1. From Figure 12, it is clear that the false alarm rate is greatly reduced by the RS  
 436 threshold, leading to a higher value of AUC than the rainfall threshold. To determine the optimal  
 437 threshold that meets a balance between the hit rate and the false alarm rate, Euclidean distance of various  
 438 thresholds is compared. The rainfall threshold with the smallest distance to the perfect point is achieved  
 439 at the percentile rank of 20, where HR is 0.818 and FAR is 0.353. RS threshold has the smallest distance  
 440 when the soil wetness's critical value is defined with its 10th percentile and the rainfall's critical value  
 441 is defined with its 20th percentile, whose HR is 0.955 and FAR is 0.124. Furthermore, the optimal  
 442 threshold is also determined by restricting HR as 1 due to the danger of missed alarms. In this way, the  
 443 rainfall threshold has the best performance for the 3rd percentile case with FAR as 0.698, while the  
 444 optimal RS threshold is achieved at the 10th percentile for both soil wetness and rainfall component,  
 445 with FAR is 0.188. Through comparing these two types of the optimal thresholds, it is found that the  
 446 prediction performance of the optimal RS thresholds is closer to the perfect point, compared with the  
 447 optimal rainfall thresholds, indicating the application of  $API_m$  in landslide prediction studies is effective  
 448 by indicating antecedent soil moisture conditions of the landslide occurrence.



449

450 Figure 12. Receiver operator characteristic (ROC) curves for rainfall thresholds and RS thresholds  
 451 whose soil wetness's critical value is determined with the 10th percentile, as well as the area under the  
 452 curve (AUC) listed.

453 Table 1. The prediction results for various thresholds in terms of TP, FN, FP, FN, HR, FAR and the  
 454 Euclidean distance (d). The optimal results are shown in bold.

455 a) Rainfall thresholds

P	$E = \alpha \cdot D^\gamma$		TP	FN	FP	TN	HR	FAR	d
	$\alpha$	$\gamma$							
1	4.33	0.30	22	0	612	172	1.000	0.781	0.781
2	5.29	0.30	22	0	575	209	1.000	0.733	0.733
3	6.01	0.30	22	0	547	237	<b>1.000</b>	<b>0.698</b>	<b>0.698</b>
4	6.61	0.30	20	2	518	266	0.909	0.661	0.667
5	7.15	0.30	20	2	499	285	0.909	0.636	0.643
6	7.64	0.30	20	2	475	309	0.909	0.606	0.613
7	8.11	0.30	20	2	462	322	0.909	0.589	0.596
8	8.54	0.30	20	2	444	340	0.909	0.566	0.574
9	8.96	0.30	20	2	428	356	0.909	0.546	0.553
10	9.35	0.30	20	2	416	368	0.909	0.531	0.538
20	12.94	0.30	18	4	277	507	<b>0.818</b>	<b>0.353</b>	<b>0.397</b>
50	24.10	0.30	4	18	71	713	0.182	0.091	0.823

456

457 b) RS thresholds

P for R	Threshold value		TP	FN	FP	TN	HR	FAR	d
	S(P10)	R (mm)							
1	0.58	0.58	22	0	2456	6267	1.000	0.282	0.282
2	0.58	1.03	22	0	2256	6467	1.000	0.259	0.259
3	0.58	1.72	22	0	2114	6609	1.000	0.242	0.242
4	0.58	2.45	22	0	1974	6749	1.000	0.226	0.226
5	0.58	2.60	22	0	1971	6752	1.000	0.226	0.226
6	0.58	2.74	22	0	1937	6786	1.000	0.222	0.222
7	0.58	3.63	22	0	1796	6927	1.000	0.206	0.206
8	0.58	4.01	22	0	1737	6986	1.000	0.199	0.199
9	0.58	4.58	22	0	1691	7032	1.000	0.194	0.194
10	0.58	5.14	22	0	1644	7079	<b>1.000</b>	<b>0.188</b>	<b>0.188</b>
20	0.58	12.60	21	1	1079	7644	<b>0.955</b>	<b>0.124</b>	<b>0.132</b>
50	0.58	36.00	16	6	338	8385	0.727	0.039	0.275

458

## 459 **5 Discussion**

460 The modified version of API proves to be more correlated with the observed soil moisture compared  
461 with the conventional version, as it is more in line with the physical process. Since the formulation of  
462 the modified API is simple and the input data is less demanding than the commonly used hydrological  
463 models, it is easier to be used in practical issues. One major challenge with its application is the  
464 determination of parameters. In this study, the calibration method is used to estimate the parameters.  
465 However, this approach is only applicable to sites with the observed soil moisture data. For sites with  
466 the in-situ measured soil moisture with limited temporal coverage, the calculation of  $API_m$  with the  
467 calibrated parameters would be useful for the data extension, as the temperature and rainfall data are  
468 always available for a long-term period. For sites without in-situ measurements of soil moisture,  
469 although the parameter extrapolation is an approach to help estimate parameters, the performance of  
470 parameters estimated in this way varies greatly, which can be seen from Figure 8. Using the satellite  
471 soil moisture as a proxy of the in-site measured soil moisture to calibrate parameters could be another  
472 way, however, the uncertainties associated with the remote sensed data may affect the parameter  
473 calibration. For the purpose of better applying  $API_m$  to practical issues, the determination of the  
474 parameters needs further exploration. For instance, when the in-situ measurements of soil moisture are  
475 sufficient, some relationships could be constructed between the calibrated parameters and  
476 characteristics of different locations. In this way, the parameters could be extrapolated to ungauged sites  
477 based on these relationships, thus the application of  $API_m$  will not be restricted by the determination of  
478 parameters.

479 The  $API_m$  provides a useful and effective indicator for soil moisture conditions. Although it is not able  
480 to estimate the absolute soil moisture value, its good correlation with the observed soil moisture data  
481 demonstrates it could capture the temporal evolution of soil moisture conditions. As a result, using  
482  $API_m$  as an indicator of soil moisture conditions could provide a proxy of soil moisture for some  
483 applications, where only the general soil moisture conditions are required rather than the absolute soil  
484 water content values. The landslide early warning is one of those applications, in which  $API_m$  could be  
485 used as an index of the antecedent soil moisture conditions before landslide occurrence. Moreover, for  
486 those explorations that investigate the effect of the soil moisture conditions on the catchment runoff  
487 response,  $API_m$  is also useful.

488 In this study, an investigation on the application of  $API_m$  in landslide studies was performed. The  $API_m$   
489 dataset for the landslide-prone area was derived with the parameters calibrated in the San Pietro  
490 Capofiume site, although the parameter extrapolation shows different reliability for different locations,  
491 the  $API_m$ 's correlation with the CCI-SM dataset is generally acceptable, since there are uncertainties  
492 associated with the satellite soil moisture data. In this application,  $API_m$  was used to index antecedent  
493 soil moisture conditions, and then employed to construct RS threshold which consists of the recent 3-  
494 day rainfall component and the antecedent soil wetness component. Direct comparison between RS  
495 threshold and rainfall threshold confirms that RS threshold is able to provide better prediction  
496 capabilities in terms of higher hit rate and lower false alarm rate. One possible reason for this  
497 improvement is that RS threshold takes into account the antecedent soil moisture conditions, which are  
498 widely recognized as the important factor in the initiation of landslides. As a result, it is inferred that  
499  $API_m$  is feasible to indicate the soil moisture condition. It is noted although RS threshold considers  
500 antecedent soil moisture conditions, the only required data is the rainfall data, therefore, RS threshold  
501 used in this study could facilitate the integration of the rainfall forecasts and fulfil predicting landslide  
502 occurrence in advance for the following day.

## 503 **6 Conclusion**

504 In this study, API is modified by incorporating more considerations of the hydrological process. First,  
505 the recession coefficient is allowed to vary with the change of temperature, and thus more consistent  
506 with the physical process of water loss. Second, the value of API is restricted by a maximum value of  
507 API to avoid overestimating the soil moisture. The added parameters are determined and validated by  
508 comparing the  $API_m$  dataset with the in-situ measured soil moisture. The better correlation between  
509 these two datasets demonstrates that  $API_m$  could better indicate the soil moisture condition, compared  
510 with  $API_c$ . This capability was further explored by applying  $API_m$  to landslide prediction studies. The  
511  $API_m$  was calculated for the landslide-prone area in the Emilia-Romagna region, northern Italy, which  
512 is used to indicate the antecedent soil moisture condition when constructing RS thresholds. RS threshold  
513 shows an improved prediction performance than the rainfall threshold, with a higher hit rate and lower

514 false alarm rate. This improvement was the result of accounting for the antecedent soil moisture  
515 condition, further indicating the validation of  $API_m$  to indicate the soil moisture condition.

516 The results reported here demonstrate the effectiveness of the modifications proposed to the  
517 conventional version of API, which improves the performance of API to indicate the soil moisture  
518 condition. Although the parameters of the modified API need to be calibrated for different locations,  
519 the simple formulation and easy availability of the required data make it more practical in some  
520 applications, through providing an effective proxy of soil moisture. In order to better apply the modified  
521 API to practical issues, more explorations are encouraged to test and improve its performance.

## 522 **Acknowledgements**

523 The authors acknowledge Dr. Matteo Berti for providing landslides data and Arpa Emilia-Romagna  
524 organization for providing the meteorological data. The first author would like to thank the China  
525 Scholarship Council for funding her study in the University of Bristol. This study is supported by the  
526 National Natural Science Foundation of China (41871299), Resilient Economy and Society by  
527 Integrated SysTems modelling (RESIST) (Newton Fund via Natural Environment Research Council  
528 (NERC) and Economic and Social Research Council (ESRC) (NE/N012143/1)) and the Fundamental  
529 Research Funds for the Central Universities of China (2016B42014).

## 530 **References**

- 531 Bolten JD, Crow WT, Zhan X, Jackson TJ and Reynolds CA (2010) Evaluating the utility of remotely  
532 sensed soil moisture retrievals for operational agricultural drought monitoring. *IEEE Journal of*  
533 *Selected Topics in Applied Earth Observations and Remote Sensing* 3: 57-66. doi:  
534 10.1109/jstars.2009.2037163
- 535 Brocca L, Melone F, Moramarco T, Wagner W, Naeimi V, Bartalis Z and Hasenauer S (2010)  
536 Improving runoff prediction through the assimilation of the ascat soil moisture product. *Hydrology*  
537 *and Earth System Sciences* 14: 1881-1893. doi: 10.5194/hess-14-1881-2010
- 538 Brocca L, Morbidelli R, Melone F and Moramarco T (2007) Soil moisture spatial variability in  
539 experimental areas of central italy. *Journal of Hydrology* 333: 356-373. doi:  
540 10.1016/j.jhydrol.2006.09.004
- 541 Brunetti M, Peruccacci S, Rossi M, Luciani S, Valigi D and Guzzetti F (2010) Rainfall thresholds for  
542 the possible occurrence of landslides in italy. *Natural Hazards and Earth System Sciences* 10: 447-  
543 458.
- 544 Castillo V, Gomezplaza A and Martinezmena M (2003) The role of antecedent soil water content in the  
545 runoff response of semiarid catchments: A simulation approach. *Journal of Hydrology* 284: 114-130.  
546 doi: 10.1016/s0022-1694(03)00264-6

547 Chleborad AF, Baum RL, Godt JW and Powers PS (2008) A prototype system for forecasting landslides  
548 in the seattle, washington, area. *Reviews in Engineering Geology* 20: 103-120. doi:  
549 10.1130/2008.4020(06)

550 Crow W, Bindlish R and Jackson T (2005) The added value of spaceborne passive microwave soil  
551 moisture retrievals for forecasting rainfall-runoff partitioning. *Geophysical Research Letters* 32.

552 Crozier M and Eyles R (1980) Assessing the probability of rapid mass movement. Third Australia-New  
553 Zealand conference on Geomechanics: Wellington, May 12-16, 1980, Institution of Professional  
554 Engineers New Zealand, pp 2

555 Draper CS, Walker JP, Steinle PJ, de Jeu RAM and Holmes TRH (2009) An evaluation of amsr-e  
556 derived soil moisture over australia. *Remote Sensing of Environment* 113: 703-710. doi:  
557 10.1016/j.rse.2008.11.011

558 Entekhabi D, Reichle RH, Koster RD and Crow WT (2010) Performance metrics for soil moisture  
559 retrievals and application requirements. *Journal of Hydrometeorology* 11: 832-840. doi:  
560 10.1175/2010jhm1223.1

561 Fedora MA (1987) Simulation of storm runoff in the oregon coast range.

562 Gariano SL, Brunetti MT, Iovine G, Melillo M, Peruccacci S, Terranova O, Vennari C and Guzzetti F  
563 (2015) Calibration and validation of rainfall thresholds for shallow landslide forecasting in sicily,  
564 southern italy. *Geomorphology* 228: 653-665. doi: 10.1016/j.geomorph.2014.10.019

565 Glade T, Crozier M and Smith P (2000) Applying probability determination to refine landslide-  
566 triggering rainfall thresholds using an empirical “antecedent daily rainfall model”. *Pure and Applied*  
567 *Geophysics* 157: 1059-1079.

568 Gruhier C, Rosnay Pd, Hasenauer S, Holmes T, De Jeu R, Kerr Y, Mougin E, Njoku E, Timouk F and  
569 Wagner W (2009) Soil moisture active and passive microwave products: Intercomparison and  
570 evaluation over a sahelian site.

571 Ibsen M-L and Casagli N (2004) Rainfall patterns and related landslide incidence in the porretta-vergato  
572 region, italy. *Landslides* 1: 143-150.

573 Jackson TJ, Cosh MH, Bindlish R, Starks PJ, Bosch DD, Seyfried M, Goodrich DC, Moran MS and Du  
574 J (2010) Validation of advanced microwave scanning radiometer soil moisture products. *IEEE*  
575 *Transactions on Geoscience and Remote Sensing* 48: 4256-4272. doi: 10.1109/tgrs.2010.2051035

576 Kerr YH, Waldteufel P, Wigneron J-P, Delwart S, Cabot F, Boutin J, Escorihuela M-J, Font J, Reul N,  
577 Gruhier C, Juglea SE, Drinkwater MR, Hahne A, Martín-Neira M and Mecklenburg S (2010) The



578 smos mission: New tool for monitoring key elements of the global water cycle. Proceedings of the  
579 IEEE 98: 666-687. doi: 10.1109/jproc.2010.2043032

580 Koster RD, Dirmeyer PA, Guo Z, Bonan G, Chan E, Cox P, Gordon C, Kanae S, Kowalczyk E and  
581 Lawrence D (2004) Regions of strong coupling between soil moisture and precipitation. *Science*  
582 305: 1138-1140.

583 Koster RD, Guo Z, Yang R, Dirmeyer PA, Mitchell K and Puma MJ (2009) On the nature of soil  
584 moisture in land surface models. *Journal of Climate* 22: 4322-4335. doi: 10.1175/2009jcli2832.1

585 Koster RD, Mahanama SPP, Livneh B, Lettenmaier DP and Reichle RH (2010) Skill in streamflow  
586 forecasts derived from large-scale estimates of soil moisture and snow. *Nature Geoscience* 3: 613-  
587 616. doi: 10.1038/ngeo944

588 Linsley RK, Kohler MA and Paulhus JL (1949) *Applied hydrology*. The McGraw-Hill Book Company,  
589 Inc.; New York,

590 Martelloni G, Segoni S, Fanti R and Catani F (2011) Rainfall thresholds for the forecasting of landslide  
591 occurrence at regional scale. *Landslides* 9: 485-495. doi: 10.1007/s10346-011-0308-2

592 Melillo M, Brunetti MT, Peruccacci S, Gariano SL and Guzzetti F (2014) An algorithm for the objective  
593 reconstruction of rainfall events responsible for landslides. *Landslides* 12: 311-320. doi:  
594 10.1007/s10346-014-0471-3

595 Mirus BB, Becker RE, Baum RL and Smith JB (2018) Integrating real-time subsurface hydrologic  
596 monitoring with empirical rainfall thresholds to improve landslide early warning. *Landslides* 15:  
597 1909-1919. doi: 10.1007/s10346-018-0995-z

598 Posner AJ and Georgakakos KP (2015) Soil moisture and precipitation thresholds for real-time  
599 landslide prediction in el salvador. *Landslides* 12: 1179-1196. doi: 10.1007/s10346-015-0618-x

600 Rossi M, Witt A, Guzzetti F, Malamud BD and Peruccacci S (2010) Analysis of historical landslide  
601 time series in the emilia-romagna region, northern italy. *Earth Surface Processes and Landforms* 35:  
602 1123-1137. doi: 10.1002/esp.1858

603 Scheevel CR, Baum RL, Mirus BB and Smith JB (2017) Precipitation thresholds for landslide  
604 occurrence near seattle, mukilteo, and everett, washington. Open-File Report, Reston, VA, pp 60

605 Staley DM, Kean JW, Cannon SH, Schmidt KM and Laber JL (2013) Objective definition of rainfall  
606 intensity–duration thresholds for the initiation of post-fire debris flows in southern california.  
607 *Landslides* 10: 547-562.

- 608 Valenzuela P, Domínguez-Cuesta MJ, Mora García MA and Jiménez-Sánchez M (2017) Rainfall  
609 thresholds for the triggering of landslides considering previous soil moisture conditions (asturias,  
610 nw spain). *Landslides* 15: 273-282. doi: 10.1007/s10346-017-0878-8
- 611 Wagner W, Naeimi V, Scipal K, de Jeu R and Martínez-Fernández J (2006) Soil moisture from  
612 operational meteorological satellites. *Hydrogeology Journal* 15: 121-131. doi: 10.1007/s10040-006-  
613 0104-6
- 614 Zêzere J, Vaz T, Pereira S, Oliveira S, Marques R and Garcia R (2015) Rainfall thresholds for landslide  
615 activity in portugal: A state of the art. *Environmental Earth Sciences* 73: 2917-2936.
- 616 Zêzere JL, Trigo RM and Trigo IF (2005) Shallow and deep landslides induced by rainfall in the lisbon  
617 region (portugal): Assessment of relationships with the north atlantic oscillation. *Natural Hazards  
618 and Earth System Science* 5: 331-344.
- 619